

—Originals—

Value of magnetization transfer contrast as a sensitive technique to reflect histopathological changes in the white matter adjacent to the frontal horns of lateral ventricles

Madoka Nakahara¹⁾, Hiromitsu Hayashi¹⁾, Tatsuo Kumazaki¹⁾ and Osamu Mori²⁾

¹⁾Department of Radiology, Nippon Medical School

²⁾Department of Pathology, Nippon Medical School

Abstract

The purpose of this study is to evaluate the usefulness of magnetization transfer contrast (MTC) as a technique to reflect histopathological changes in the white matter adjacent to the frontal horns of the lateral ventricles. Radiological-pathological correlation was performed in six patients who underwent Magnetic Resonance (MR) examination prior to death and in whom post-mortem examinations of the brain were obtained. The extent and the severity of degeneration in the white matter adjacent to the frontal horns were evaluated histopathologically, and compared with those observed on the conventional proton density (PD) weighted MR images (Group 1). Changes in the white matter of another 35 patients were classified into three types according to the pattern of high signals adjacent to the frontal horns on conventional PD weighted MR images, and magnetization transfer ratio (MTR) in the white matter adjacent to the frontal horns was calculated from multi-slice and single-slice FSE images (Group 2). The relationship between signal intensities and MTR in the white matter adjacent to the frontal horns was evaluated.

The extent of degeneration in the white matter adjacent to the frontal horns was classified into mild, moderate and severe types on the basis of stainin for myelins, axons and astrocytes. In Group 1, histopathological findings indicated a difference in severity of degeneration in the white matter adjacent to the frontal horns among the three types, while no significant differences were noted in the signals on PD weighted MR images. In Group 2, MTR showed significant differences in the signal intensities in the white matter adjacent to the frontal horns ($p < 0.01$) between the three types, while conventional PD weighted MR images failed to differentiate between them.

In conclusion, MT imaging is a sensitive technique to evaluate the histopathological changes in the white matter adjacent to the frontal horns that cannot be detected by conventional MR imaging. (J Nippon Med Sch 1999; 66: 245 – 252)

Key words: magnetization transfer contrast, magnetization transfer ratio, reactive astrocyte

Introduction

The white matter just adjacent to the frontal horns of lateral ventricles is visualized as various differently shaped areas of high signal intensity on conventional

T2 weighted and PD weighted MR images. There have been previous investigations of these high signals in the white matter in comparison with the results of histopathological analyses¹⁻⁴. High signals in the white matter were reported to reflect various pathological conditions such as atrophic demyelina-

tion, cerebral ischemia or infarction¹⁻⁴. However, the association of specific histopathological findings with high signal intensities on conventional MR images is still uncertain. Conventional MR imaging can only evaluate the morphological changes in areas with high signal intensity, but it lacks specificity to reflect the histopathological changes in the white matter.

MTC first reported by Wolff and Balban⁵ is a new technique to reflect tissue contrast. As MTC reflects the tissue contrast based on the interaction between highly mobile protons and immobile restricted protons⁶⁻⁹, it is expected to provide precise and specific information about tissue characteristics that conventional MR imaging cannot provide. The aim of this study is to evaluate the usefulness of MTC as a sensitive technique to reflect the histopathological changes in the white matter adjacent to the frontal horns of the lateral ventricles that cannot be detected by conventional MR imaging.

Materials and Methods

Radiological-pathological correlation study

Four men and two women, 37 to 88 years old (mean, 67 years), with no known central nervous system (CNS) disease were examined. They underwent brain MR examinations prior to death and postmortem examinations of their brains were also performed. MR imaging was performed with 1.5 T unit (Signa Horizon; GE Medical Systems, Milwaukee, WI) using a head coil. T 1 weighted spin-echo (SE) (TR 500/TE 10), T 2 weighted FSE (TR/effective TE/NEX=3500/100/1) and PD weighted FSE images (2000/15/1) were acquired in the axial plane with an echo train length of 4, field of view of 24 cm, slice thickness of 6.5 mm, slice gap of 2 mm and imaging matrix of 256 × 256. The interval between MR examination and postmortem examination was 25 to 128 days. The shape of the high signal intensity area of the white matter adjacent to the frontal horns on PD weighted FSE images was evaluated by two radiologists.

Fixed specimens of the brains were cut into axial slices with reference to the MR images obtained in life. A neuropathologist and a radiologist (M.N.) inspected the slices and carefully selected those exhibiting white matter just adjacent to the frontal horns,

which corresponded to the high signal intensity on MR images, for microscopic sectioning. To study the extent and severity of white matter degeneration, the white matter of 12 hemispheres from six patients was stained by the Kluver-Barrera (K-B) method for myelin, the Bodian silver method for axons, and the peroxidase-antiperoxidase immuno-histologic method for glial fibrillary acidic protein (GFAP, cow polyclonal, 1: 100 DACO Z 334) of astrocytes. GFAP was detected with biotinylated secondary antibody coupled with hoarse radish peroxidase and visualized with DAB (diaminobenzidine) to specify and evaluate astrocytosis¹⁰. First, microscopic findings of each sample of white matter surrounding the frontal horns were classified into three groups, i. e. mild, moderate and severe types, according to the extent of degeneration. Second, all the specimens of white matter about 2~5 mm from the contour of the frontal horns were examined for the severity of degeneration among the three types. The ependymitis granularis which lay in the rim of the frontal horns of the lateral ventricles was excluded from the histopathological study¹⁻². The relationship between signal intensities on conventional PD weighted MR images and histopathological changes in the white matter adjacent to the frontal horns was evaluated.

Magnetization transfer contrast study

Brain MR examinations were performed in a total of 303 adult patients from Jul. ~Sept. 1997. Nine of these 303 patients were excluded because of interference by motion artifacts. Of the remaining 294 patients, those with stroke (n=69), cerebral hemorrhage (n=12), brain tumor (n=64), vascular malformation (n=34), trauma (n=14), demyelinating diseases (n=11), infection (n=4) or extra-axial hemorrhage (n=9) were excluded from the present study. Patients suffering from cerebrovascular risk factors (hypertension, hyperlipemia and diabetes) (n=42) were also excluded. The remaining 35 patients with no evidence of cerebral nervous system disease (23 men and 12 women), aged 21 to 87 years old with a mean age of 56 years, were included in this study. Eight hemispheres from 35 patients were, however, excluded because of inappropriate setting of the imaging plane. Therefore, a total of 62 hemispheres from 35 patients

were finally examined in this MTC study.

All MR studies were performed with 1.5 T units (Signa Horizon; GE Medical Systems) using a head coil. Before the MTC study, MR images were obtained using the same protocols as the radiological-pathological correlation study. Subsequently, MTC analysis using multi-slice and single-slice FSE imaging (1500/15/1), with an echo train length of 4, field of view of 24 cm, slice thickness of 5 mm, slice gap of 5 mm, and imaging matrix of 256×256 , was carried out. Fifteen multi-slice FSE images were obtained in the axial plane with the central slice set at the level of the base of the third ventricle. Single-slice FSE images were obtained at the same level as the central slice on multi-slice FSE imaging. Radio frequency (RF) transmission and reception gains were kept constant for multi-slice and single-slice acquisitions.

The shape of the high signal intensity area of the white matter adjacent to the frontal horns was evaluated by two radiologists and classified into three types, i. e. triangular, oval, and irregular, on conventional PD weighted MR images. MTR was calculated by the following formula with the measured signal intensity of both the central slice of multi-slice FSE images and single-slice FSE images.

$$\text{MTR} = \text{MS} - \text{MM} / \text{MS}$$

MS: signal intensity of single-slice FSE

MM: signal intensity of multi-slice FSE

The region of interest (ROI) for calculating MTR was set at the white matter about 2~3 mm from the contour of the frontal horns to avoid inclusion of the signal intensity of cerebrospinal fluid. The size of ROI was 5~7 mm². To ensure accurate localization and consistency of measurement, these ROIs were carefully placed by one radiologist. The position, shape and size of ROI were fixed between multi-slice and single-slice FSE images using the console of the MR imager. MTR was compared among the three types. The relationship between the signal intensities and MTR in the white matter adjacent to the frontal horns was evaluated.

Statistical analysis

The nonparametric Kruskal-Wallis test and Scheffe's F test were used to compare MTR between the types. Probability (p) values of less than 0.05 were considered significant.

Results

Radiological-pathological correlation study

Histopathological findings were classified into mild (**Figs. 1-A, B, C, D; n=4**), moderate (n=4), and severe types (**Figs. 2-A, B, C, D; n=4**) according to the extent of degeneration of the white matter. A triangular-shaped myelin pallor region was consistently seen in the K-B stain just adjacent to the frontal horns in all three types (**Figs. 1-A, 2-A**) with a base of 5.6 ± 0.35 (SD) mm and height of 5.8 ± 0.26 (SD) mm. The mild type showed slightly decreased myelin content only in the small triangular region just adjacent to the frontal horns. No axonal loss or increase in number of reactive astrocytes were seen in the white matter (**Figs. 1-A, B, C, D**). The moderate type showed decreased myelin content and axonal loss with many reactive astrocytes in the triangular region and in the white matter just outside the triangular region. These changes were observed in the genu of corpus callosum beyond the triangular region but not in the subcortical white matter. In the severe type, decreased myelin content and axonal loss with many reactive astrocytes were seen in the triangular region and spread further into the genu of corpus callosum or subcortical white matter (**Figs. 2-A, B, C, D**). The relationship between the histopathological findings and conventional PD weighted MR images of the white matter adjacent to the frontal horns is shown in **Table 1**. The extent of white matter degeneration corresponded to high signals adjacent to the frontal horns on PD weighted MR images. The mild type showed the triangular-shaped area of high signal intensity on MR images (**Fig. 1-E**). The moderate type showed an oval-shaped area of high signal intensity, while the severe type showed an irregularly shaped area with high signal intensity (**Fig. 2-E**). Despite the histopathological differences in the white matter, all the white matter specimens examined showed the same high signal intensities on conventional MR images.

Magnetization transfer contrast study

The shapes of high signals adjacent to the frontal horns were classified into triangular (**Fig. 3-A; n=40**), oval (**Fig. 3-B; n=12**) or irregular types (**Fig. 3-C;**

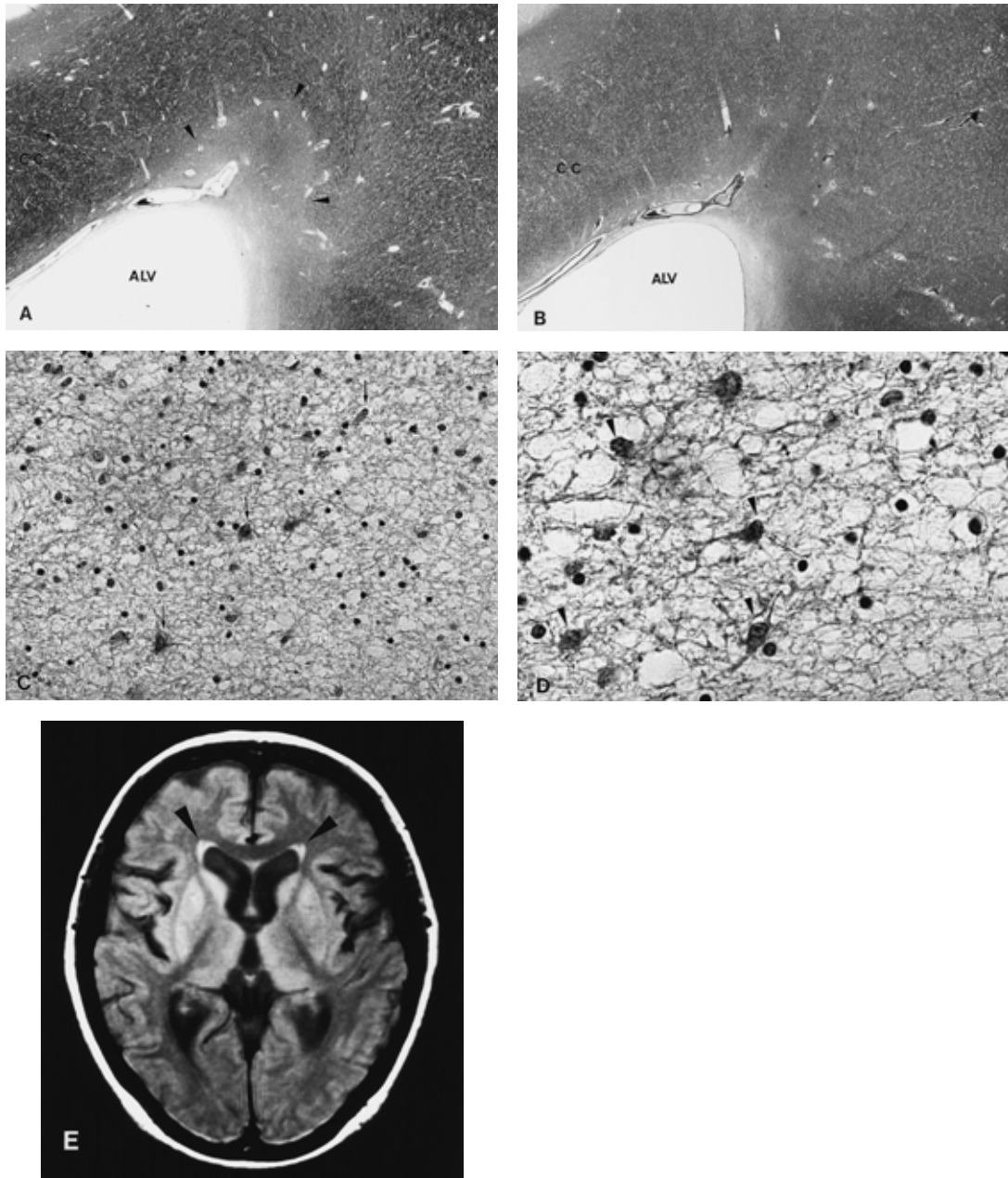


Fig. 1 Micrograph and FSE proton density MR image of the mild type white matter just adjacent to the frontal horns. A: Myelin-stained section of the white matter just adjacent to the frontal horns. Note small triangular area of myelin pallor adjacent to the frontal horns (arrowhead). cc; corpus callosum, ALV; Anterior horn of lateral ventricle Kluver-Barrera, $\times 10$. B: Axon-stained section at the same level adjacent to the frontal horns. No marked axonal loss was observed. ALV; Anterior horn of lateral ventricle Bodian silver method, $\times 10$. C: GFAP of astrocytes-stained section at the same level adjacent to the frontal horns. Normal astrocytes were seen (arrows). Immunostaining with GFAP, $\times 200$. D: With higher magnification of the astrocytes (arrowheads). Immunostaining with GFAP, $\times 400$. E: Boundaries of the area of myelin pallor correlated well with the small triangular region of high signal intensity observed on conventional PD weighted MR images (arrowheads).

n=10) on PD weighted images. The triangular type showed a tiny triangular area of high signal intensity comprised of the rim of the frontal horn as the base, the genu of corpus callosum as the medial side, and

some radiations terminating posteriorly in the frontal lobe as the lateral side. The width of the high signal intensity area was almost equivalent to or smaller than those of the frontal horns of lateral ventricles. The

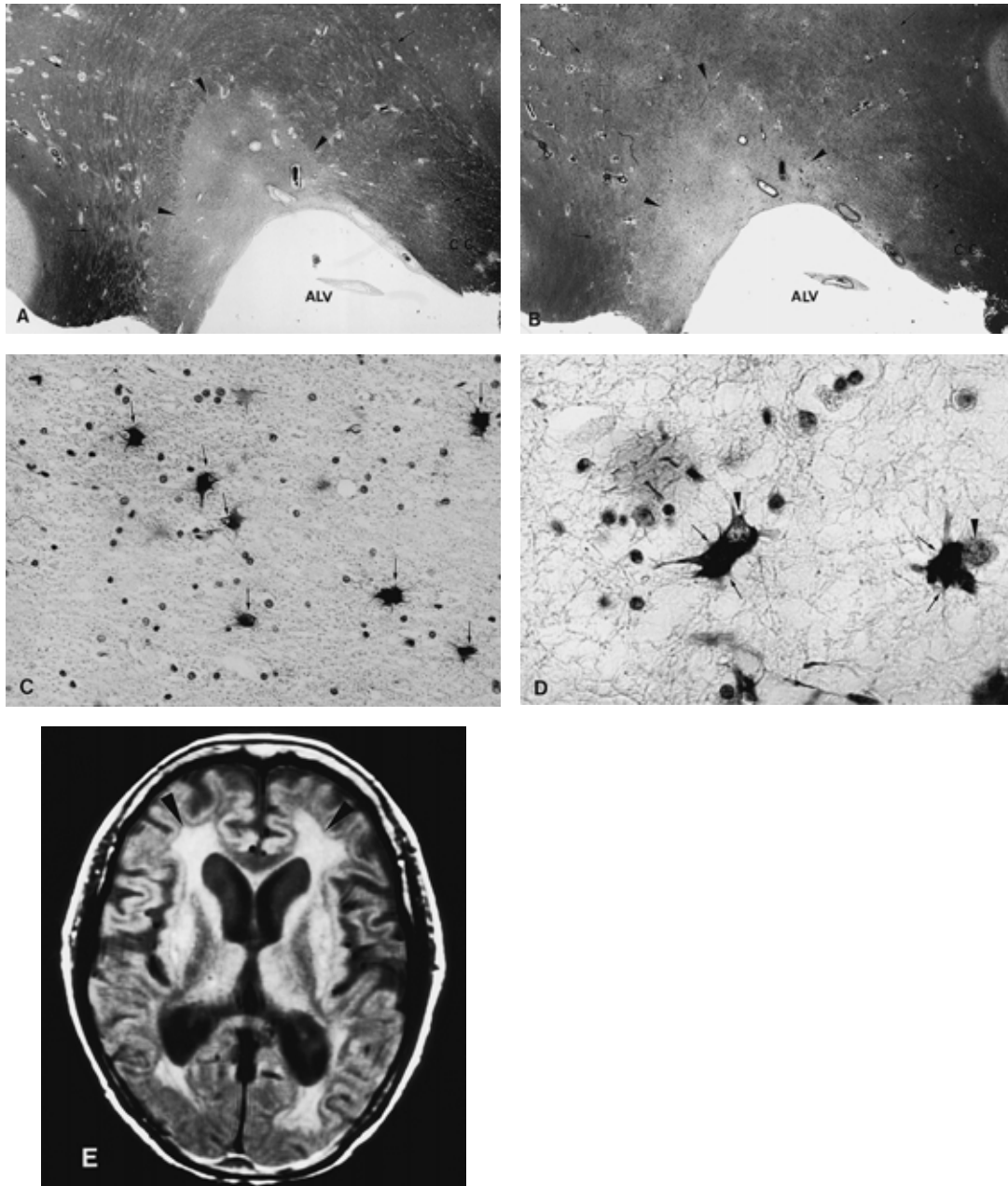


Fig. 2 Micrograph and FSE proton density MR image of the severe type white matter surrounding the frontal horns. A: Myelin-stained section of the white matter just adjacent to the frontal horns. Note small triangular myelin pallor just adjacent to the frontal horns (arrowhead) and decreased myelin content extending around the triangular pallor and corpus callosum (arrows). cc; corpus callosum, ALV; Anterior horn of lateral ventricle Kluver-Barrera, $\times 10$. B: Axon-stained section at the same level adjacent to the frontal horns. The same small triangular region showing axonal loss adjacent to the frontal horns (arrowhead) was seen. Mild axonal loss extended around the triangular pallor and corpus callosum (arrows). ALV: Anterior horn of lateral ventricle Bodian silver method, $\times 10$. C: GFAP of astrocytes-stained section at the same level adjacent to the frontal horns. Many reactive astrocytes strongly positive GFAP were seen (arrows). Immunostaining with GFAP, $\times 200$. D: With higher magnification of the reactive astrocyte. Large nucleus (arrowhead) and hypertrophic cytoplasm (arrows) were seen. Immunostaining with GFAP, $\times 400$. E: Boundaries of the area of myelin pallor and axonal loss correlated well with the large irregularly shaped region of high signal intensity observed on conventional PD weighted MR images (arrowhead).

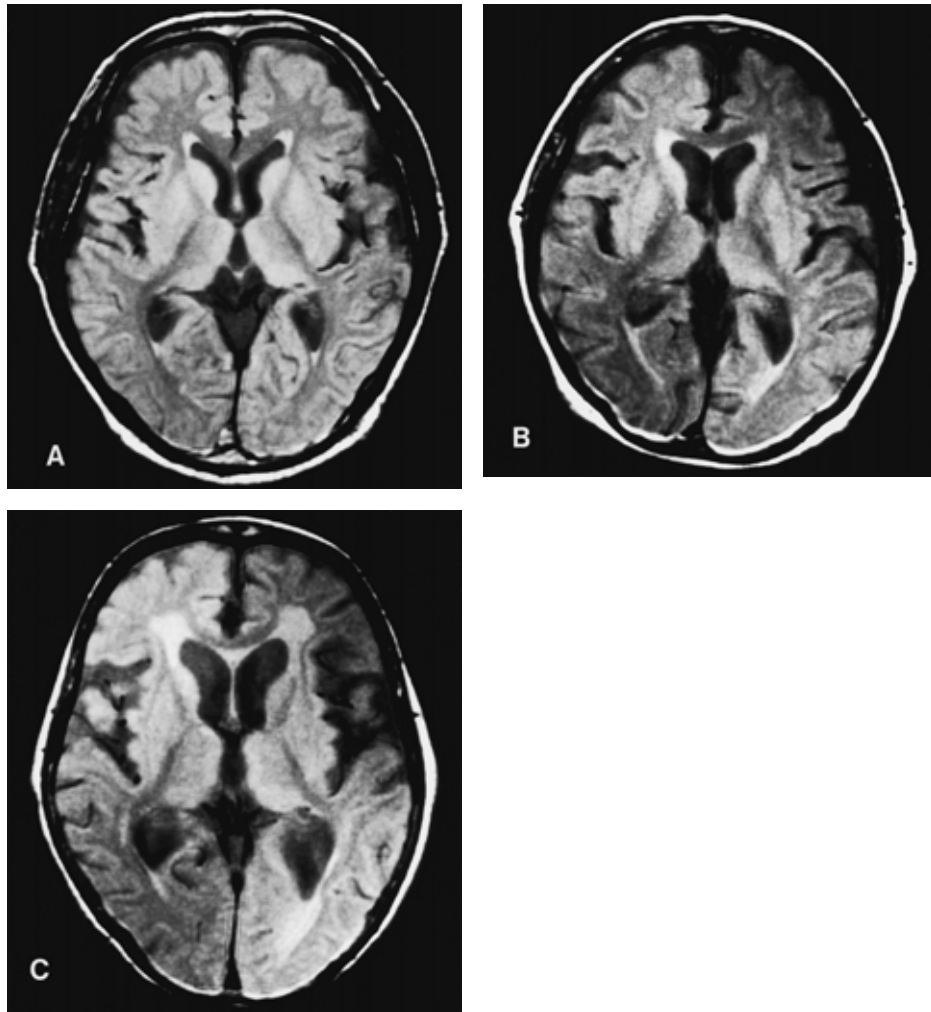


Fig. 3 White matter surrounding the frontal horns on FSE proton density weighted MR images. A: Triangular type; The triangular-shaped high signal intensity region is depicted just adjacent to the frontal horns bilaterally. B: Oval type; Oval-shaped high signal intensity region is depicted surrounding the frontal horns bilaterally. The area of high signal intensity extended into the white matter beyond the triangular-shaped high signal intensity region but not into the subcortical white matter. C: Irregular type; Irregularly shaped high signal intensity region surrounding the frontal horns bilaterally. The high signal intensity extended into the corpus callosum or subcortical white matter.

oval type showed small oval areas with high signal intensity. The width of high signal intensity was a little greater than that of the frontal horns. The irregular type showed diffuse confluent high intensity signals spread in several random directions from the rim of the frontal horn to the subcortical white matter. The width of high signal intensity areas was greater than that of the frontal horns. While the white matter just adjacent to the frontal horns of the three types showed the same high signals on conventional PD weighted images, MTR of those in the oval and irregular type was significantly lower than that in the triangular type ($p < 0.01$) (Table 2).

Discussion

In the present study, histopathological examination revealed a small triangular myelin pallor region just adjacent to the frontal horns in all cases. This region, referred to here as *the triangle*, was observed in the white matter just adjacent to the frontal horns regardless of the shape of high signals on conventional PD weighted images. To our knowledge, there have been no previous reports of detailed investigation of the existence of *the triangle*. While *the triangle* had a common shape and size in all cases, the state of mye-

Table 1 Radiological-pathological correlation of the white matter just adjacent to the frontal horns

	Histopathological classification		
	Mild type (n=4)	Moderate type (n=4)	Severe type (n=4)
Degeneration in the white matter			
Extent			
Triangular region	+	+	+
Genu of corpus callosum	-	+	+
Subcortical white matter	-	-	+
Severity			
Decreased myelin content	+	+	+
Axonal loss	-	+	+
The number of reactive astrocytes	few	many	many
Conventional MR image			
Shape of signal intensity	Triangle	Oval	Irregular
Signal intensity	high	high	high

Note. + means presence of decreased myelin content or axonal loss, - means absence of decreased myelin content or axonal loss.

Table 2 Mean magnetization transfer ratio(%MTR) of three types

	Triangular type n=40	Oval type n=12	Irregular type n=10
%MTR			
Mean (sd)	23.7(2.4)	19.5(2.5)	17.6(2.3)

Note. %MTR : Magnetization transfer ratio $\times 100$.

** : $p < 0.01$ comparison with Triangular type

lin, axons and astrocytes varied among the three types. The most important histopathological difference in *the triangle* among the three types was the presence or absence of axonal loss with many reactive astrocytes.

Many reactive astrocytes were observed in regions showing axonal loss on histopathological examination¹⁰⁻¹³. The number of reactive astrocytes increases when brain damage occurs regardless of the cause¹⁰⁻¹³. Reactive astrocytes have a large nucleus and hypertrophic cytoplasm containing large amounts of GFAP¹⁰⁻¹³, so an increase in the number of reactive astrocytes has the potential to increase macromolecule production. On the other hand, the presence of reactive astrocytes causes enlargement of the extracellular space¹⁰⁻¹³, which then becomes filled with fluid. Therefore, increases in number of reactive astrocytes may also result in increases in the volume of the extracellular fluid¹⁰⁻¹². These structural changes and increases in number of reactive astrocytes may result in a strong interaction between the extracellular fluid and the macromolecules (nuclear protein or

GFAP).

The interaction between free water protons and macromolecular protons determines the amount of magnetization transfer effect; that is, the greater the interaction between the two, the more magnetization transfer effect occurs. In our MTC study, ROIs for the measurement of MTC were within or corresponded to *the triangle*, considering the size and location of the ROI of MTR. MTR of the white matter adjacent to the frontal horns in the oval or the irregular type was significantly lower than that in the triangular type. This result suggested that there was a greater magnetization transfer effect in the white matter of the oval or irregular type than in the triangular type. The decrease in MTR of the white matter in the oval or irregular type reflected our histopathological findings, mainly the increased number of reactive astrocytes. The observation in this study that the decreased MTR in areas of the white matter adjacent to the frontal horns showing high signal intensity was related to the increased number of reactive astrocytes corresponded to the previous report¹⁴. High signals in the white matter adjacent to the frontal horns corresponded to the extent of degeneration of the white matter in this histopathological study. However, there were no differences in the signal intensities in the white matter among the three types. Conventional MR imaging is a sensitive method to determine the extent of degeneration of the white matter but it fails to differentiate the severity in the different types. In

contrast, MTR could differentiate between the high signals in the white matter adjacent to the frontal horns among the three types. Our results are consistent with the idea that MTR reflects the microscopic changes in the white matter adjacent to the frontal horns better than conventional MR imaging.

MTC is commonly achieved by using off-resonance radio frequency pulses or by using conventional multi-slice SE or multi-slice FSE images¹⁵⁻¹⁸. PD weighted FSE sequences showed some advantages for obtaining MTC in the present study; i. e. it was easy to detect small lesions depicted as high signal intensities, and accurately place ROI at the lesions. However, this method was limited in that only a single imaging plane could be used to evaluate MTC. We did not perform a detailed comparative study between the results of histopathological examinations and MTR in this investigation. Prospective studies with direct comparison of histopathological findings and MTR are necessary to clarify the clinical significance of MTR of the white matter.

Conclusion

This study indicated that MTC is a sensitive technique to reflect the histopathological changes in the white matter that cannot be determined from conventional MR images.

Acknowledgments: The authors thank C. Kim, MD, Ph. D., for statistical analysis. We are also grateful to T. Tsuchihashi, T. Maki, Y. Sasaki, and S. Yoshizawa for technical assistance with MRI.

References

1. Sze G, De Armond SJ, Brant-Zawadzki M, Davis RL, Norman D, Newton TH: Foci of MRI signal (pseudo lesions) anterior to the frontal horns: histologic correlations of a normal finding. *AJR Am J Roentgenol* 1986; 147: 331—212.
2. Leifer D, Buonanno FS, Richardson EP Jr: Clinicopathologic correlations of cranial magnetic resonance imaging of periventricular white matter. *Neurology* 1990; 40: 911—918.
3. Fazekas F, Kleinert R, Offenbacher H, Schmidt R, Kleinert G, Payer F, Radner H, Lechner H: Pathologic correlates of incidental MRI white matter signal hyperintensities. *Neurology* 1993; 43: 1683—1689.
4. Kertesz A, Black SE, Tokar G, Benke T, Carr T, Nicholson L: Periventricular and subcortical hyperintensities on magnetic resonance imaging 'rims, caps, and unidentified bright objects'. *Arch Neurol* 1988; 45: 404—408.
5. Wolff SD, Balban RS: Magnetization transfer contrast (MTC) and tissue water proton relaxation in vivo. *Magn Reson Med* 1989; 10: 135—144.
6. Sappey-Marinié D: High-resolution NMR spectroscopy of cerebral white matter in multiple sclerosis. *Magn Reson Med* 1990; 15: 229—239.
7. Lundbom N: Determination of magnetization transfer contrast in tissue: An MR imaging study of brain tumor. *AJR Am J Roentgenol* 1992; 159: 1279—1285.
8. Eng J, Ceckler TL, Balban RS: Quantitative 1 H magnetization transfer imaging in vivo. *Magn Reson Med* 1991; 17: 304—314.
9. Koenig SH: Cholesterol of myelin is the determinant of gray-white contrast in MRI of brain. *Magn Reson Med* 1991; 20: 285—291.
10. Iijima S, Kageyama K, Ishikawa E, Shimamine T: Atlas of Histopathology. 3rd ed, 1987. Bunkodo Tokyo.
11. Latov N, Nilaver G, Zimmerman EA, Johnson WG, Silverman AJ, Defendini R, Cote L: Fibrillary astrocytes proliferate in response to brain injury: A study combining immunoperoxidase technique for glial fibrillary acidic protein and radioautography of tritiated thymidine. *DEV BIOL* 1979; 72: 381—384.
12. Ikuta F, Yoshida Y, Oyanagi E, Takeda S, Yamazaki K, Watabe K: Revised Pathophysiology on BBB Damage: the edema as an ingeniously provided condition for cell motility and lesion repair. *Acta Neuropathol Suppl.* 1983; VIII: 103—110.
13. Ikuta F: The process of brain lesion repair and activity of astrocytes. In: Ikuta F, ed. 1991; pp 211—231. *Neuropathology in Brain Research Elsevier Science Publishers B. V.*
14. Wong KT, Grossman RI, Boorstein JM, Lexa FJ, McGowan JC: Magnetization transfer imaging of periventricular hyperintense white matter in the elderly. *AJNR Am J Neuroradiol* 1995; 16: 253—258.
15. Dixon WT, Engels H, Castillo M, Shardashti M: Incidental magnetization transfer contrast in standard multislice imaging. *Magn Reson Imaging* 1990; 8: 417—422.
16. Kobayashi S, Takeda K, Sakuma H, Kinosada Y, Nakagawa T: Uterine Neoplasms: Magnetization transfer analysis of MR images. *Radiology* 1997; 203: 377—382.
17. Melki PS, Mulkern RV: Magnetization transfer effects in multi-slice RARE sequences. *Magn Reson Med* 1992; 24: 189—195.
18. Kinosada Y, Matushima S, Kubo H, Maeda H: Evaluation of quantitiveness in fast spin echo: Complexity of image contrast due to magnetization transfer mechanism. *Japanese-Deutsche Medizinische Berichte* 1997; 42: 7—18.

(Received, February 17, 1999)

(Accepted for publication, April 26, 1999)